HYDROGEN, FUEL CELL & ENERGY STORAGE

Investigating Numerically the Impact of Phase Change Materials on Heat Exchangers to Optimize Energy Consumption

Seyyed Amirreza Abdollahi[a,*] | **Seyyed Kazem Yekani**[a] | **Seyyed Faramarz Ranjbar**[a]

Seyyed Esmail Razavi[a] | **Mostafa Barzegar Gerdroodbary**[b]

[a] Department of Mechanical Engineering, Faculty of Mechanical Engineering, University of Tabriz, Tabriz, Iran
[b] Department of Electromechanical Engineering, C-MAST-Center for Mechanical and Aerospace Science and Technology, Universidade da Beira Interior, Covilha, Portugal

[*] Corresponding author, Email: s.a_abdollahi@yahoo.com

Article Information

Article Type
Research Article

Article History
Received: *11 Dec 2025*
Revised: *15 Feb 2026*
Accepted: *01 Mar 2026*
Published Online: *06 Mar 2026*

Keywords
Heat exchangers
Phase change material
Optimization of energy consumption
Thermal comfort

Abstract

This article presents a novel three-dimensional numerical investigation of turbulent water–air flow and displacement heat transfer in a shell-and-tube heat exchanger enhanced with paraffin phase-change material (PCM) and aluminum oxide nanoparticles. Covering Reynolds numbers from 0 to 3 000, the governing equations are solved via the finite-volume method.The study's findings indicate that employing phase-change material surrounding the tube and keeping a steady heat flux can both increase a shell and tube heat exchanger's penetration coefficient. The impact of this modification has been compared to that of a straight, circular tube, providing practical insights for heat exchanger design. The chosen fluid flow exhibits turbulence as it moves through the tube and collides with the thermal boundary layer, increasing the internal transfer coefficient of the fluid flow. The findings show an insignificant error of 8.71% for the grid independence section.

Cite this article: Abdollahi, S. A., Yekani, S. K., Ranjbar, S. F., Razavi, S. E., Barzegar Gerdroodbary, M. (2026). Investigating Numerically the Impact of Phase Change Materials on Heat Exchangers to Optimize Energy Consumption. DOI: 10.22104/hfe.2026.7415.1344

 Publisher: Iranian Research Organization for Science and Technology (IROST)
DOI: 10.22104/hfe.2026.7415.1344

1 Introduction

The investigation of methods to enhance heat transfer in heat exchangers for improved efficiency has been a primary focus across various industries, including refrigeration, air conditioning, automotive, aerospace, petrochemical, pharmaceutical, food, and thermal power plants. As the converter's efficiency increases, its size decreases, resulting in energy savings. It is also essential to consider the pressure drop when dealing with heat pipes. In other words, changes in pressure drop should be considered alongside the increase in heat transfer. This is because a reduction in pressure drop is directly proportional to the decrease in operational costs. Therefore, it can be said that one of the important reasons for investigating the methods of increasing heat transfer is the optimization of energy consumption, which has made the technology of increasing heat transfer in heat pipes attractive and important.

Fluids commonly used in industrial processes, such as water, engine oil, ethylene glycol, and mineral liquids, are crucial components in various applications such as power generation, chemical processes, cooling and heating systems, transportation, microelectronics, and other micrometer-scale applications. The inadequate heat transfer properties of these fluids pose a significant challenge in enhancing the efficiency of heat pipes. Recognizing that the thermal conductivity of solid particles is hundreds of times higher than that of fluids, an innovative approach was developed to address this issue. This involved creating a suspension of minute solid particles in pure fluids, which proved to be an effective solution for augmenting the heat transfer properties of conventional energy-carrying fluids. A slurry-shaped product can be created by adding various types of metal, non-metal, and polymer particles to the base fluid [1]. Chemically stable metals, metal oxides, and carbon-based materials are commonly used as metal particles [2]. However, suspensions containing particles in micrometer and even millimeter sizes can lead to issues such as particle abrasion, blockage of channel pathways, and erosion of pipe networks, reduced momentum transfer, and increased pressure drop [3].

In particular, the particles in the suspension tend to settle. While the slurry suspension exhibits higher thermal conductivity than the base fluids, it is still unsuitable for practical applications as an energy carrier fluid [4]. Nanofluids, which utilize nanometer-sized particles in a pure base fluid, emerged as a result of advancements in nanotechnology and proved instrumental in enhancing the heat transfer properties of fluids [5]. In comparison to suspensions containing micrometer and millimeter-sized particles, nanofluids exhibit improved stability, enhanced rheological properties, and increased thermal conductivity [6–8].

Over the years, numerous researchers have investigated and explored the heat transfer properties of various nanofluids. The methods employed to enhance heat transfer can be categorized into two main categories: (1) Active methods, and (2) Passive methods utilizing external energy sources. Active methods involve techniques such as electrostatic fields to promote mass mixing of the fluid near the heat exchange surface [9]. Other active methods include acoustic vibration (generating sound waves in the fluid), injection or suction (utilizing porous heat transfer surfaces), mechanical aids (stirring the fluid through mechanical means or rotating the pipe surface), and surface or fluid vibration (utilizing high or low frequencies to improve heat transfer) [10, 11]. Passive methods, on the other hand, do not require external energy sources but can still enhance heat transfer through various means. These include roughening the surface, utilizing extended surfaces, adding attachments, or introducing solid particles and gas bubbles into the fluid. Whether active or passive, all methods of enhancing heat transfer can be broadly categorized into two main groups: increasing heat transfer in the main flow and increasing heat transfer in the secondary flow [12, 13].

The utilization of extended surfaces represents a passive method for enhancing heat transfer in the secondary flow. Previous research conducted in this field primarily focused on studying the impact of these vortex generators on Newtonian fluids [14]. Given the extensive array of non-Newtonian fluids and their significance in heat exchangers utilized within the food, pharmaceutical, and petrochemical industries, coupled with the limited research in this area, it is imperative to explore the behavior of these fluids within exchangers [15, 16]. Additionally, owing to the low heat transfer coefficient of non-Newtonian fluids, employing techniques to enhance heat transfer, such as the addition method, can benefit this fluid type. Nanostructures represent the convergence of the tiniest man-made tools and the largest molecules found in living organisms [17, 18]. A nanostructured material refers to a crystalline solid at the nanometer scale. During the Middle Ages, glassmakers were unaware of why adding gold to glass altered its color. During this period, nanometer-sized gold particles were utilized in the production of glass for medieval churches, resulting in the creation of highly appealing colored glass. In fact, it is not so difficult to find examples for using metal nanoparticles [19, 20].

A substance that releases or absorbs enough energy during a phase transition to provide usable heat or cooling is known as a phase-change material (PCM). Usually, one of the first two fundamental states of matter – solid or liquid – will give way to the other. In non-classical states of matter, like the conformity of crystals, where the material changes from conforming to one crystalline structure to another, which may be a higher or lower energy state, there may also be a phase transition [21–24].

Our article investigates the flow and turbulence of water and air within a shell and tube heat exchanger in three dimensions. This study primarily concerns applying phase change materials (PCM) in displacement heat transfer. The paper offers a novel analysis of the changes in pressure gradient and displacement heat transfer in turbulent flow within a shell and tube heat exchanger. In addition, aluminum oxide nanoparticles and paraffin PCM with Reynolds numbers from 0 to 3000 are used for the first time.

2 Define the Problem

The study delved into three-dimensional flow, turbulence, and forced convection heat transfer in a shell and tube heat exchanger. This research examined the impact of geometrical parameters of a 600 mm long and 100 mm thick heat exchanger with two inlets and two outlets. Specifically, the first and second inlets introduced air and water, with water flowing at a velocity of 0.1 m/s and air at 1 m/s. The water and air temperatures were recorded at 353.15 K and 278.15 K, respectively, and were subsequently analysed using software. This simulation involves coupling the governing equations of continuity, momentum, and energy with the desired geometry being meshed according to the aforementioned conditions.

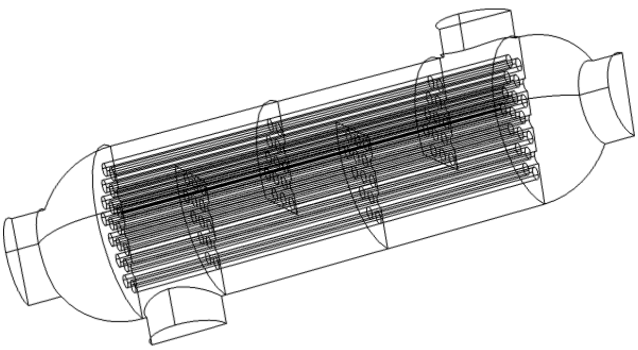

Fig. 1. Shell and tube heat exchanger

The fundamental equations governing the problem were discretized using the finite volume implicit method in second-order form, resulting in a set of algebraic equations. The iterative simple algorithm was then employed to obtain multiple solutions until the desired convergence was achieved. The simple algorithm was utilized to simultaneously solve for velocity and pressure in steady, turbulence two-dimensional flow. Specific boundary conditions were considered when calculating the horizontal interaction of forced heat transfer and flux in the common phases of the surface and nanofluid, as well as the magnetic field passing through it. The coefficients of forced heat transfer and constant flux on the surface were established by inputting graphical problems and writing text commands in Comsol software. Additionally, the properties of nanofluids at various volume percentages were computed using the mathematical formulas provided in subsection 2.1.

2.1 Equations governing fluid flow

The equation of continuity in an incompressible fluid is the term [23]:

$$\nabla \cdot \boldsymbol{u} = 0 \tag{1}$$

The momentum equation for fluid displacement flow, based on the assumptions made in the problem, is as follows [23]:

$$\rho_0 \left(\frac{\partial \boldsymbol{u}}{\partial \tau} + \boldsymbol{u} \cdot \boldsymbol{\nabla} u \right) = -\boldsymbol{\nabla} p + \boldsymbol{\nabla} S + \alpha \rho_0 (T - T_0) \boldsymbol{k} \tag{2}$$

where ρ is the density, p is the pressure, $\boldsymbol{u}$ is the velocity vector, T is the fluid temperature, S is the stress tensor, $\boldsymbol{k}$ is the unit vector for Gravity, and α the thermal expansion coefficient is included in the Equation (2) in the general state [23]:

$$S = \eta G \tag{3}$$

Equation (3) is the deformation rate tensor of a Newtonian fluid with constant viscosity. The energy equation for an incompressible fluid adheres to Fourier's modified law, and can be expressed as [23]:

$$\rho_0 \left(\frac{\partial T}{\partial \tau} + \boldsymbol{u} \cdot \boldsymbol{\nabla} T \right) = k \nabla^2 T + \eta \varphi \tag{4}$$

η is the viscosity loss.

In this study, water was used as the base fluid to which Al_2O_3 nanoparticles were added. The characteristics of base and nanofluids are shown in Table 1.

Ferrofluid density (ρ_m) is obtained from the Equation (5) [23]:

$$\rho_\mathrm{m} = (1 - \varphi)\rho_\mathrm{f} + \varphi \rho_\mathrm{p} \tag{5}$$

The coefficient of thermal expansion of ferrofluid is equal to [23]:

$$\beta_\mathrm{m} = (1 - \varphi)\beta_\mathrm{f} + \varphi \beta_\mathrm{p} \tag{6}$$

Table 1. Properties of base fluid and nanoparticle

Properties	Base fluid (Water)	PCM
C_p (J/kg.k)	4179	612
ρ (kg/m^3)	997.1	4215
K (W/m.k)	0.605	6.2
μ (kg/ms)	0.000891	-
β (k^{-1})	0.00021	13.3×10^{-6}

The Specific heat of ferrofluid (C_{pm}) is [23]:

$$C_{\mathrm{pm}} = \frac{1}{\rho_{\mathrm{m}}}\left[(1-\varphi)\rho_{\mathrm{f}}C_{\mathrm{pf}} + \varphi_{\mathrm{pp}}C_{\mathrm{pp}}\right] \quad (7)$$

The coefficient of ferrofluid thermal conductivity (k_m) is obtained from the Equation (8) [23]:

$$k_{\mathrm{m}} = k_{\mathrm{f}}\left[\frac{2 + k_{\mathrm{pf}} + 2\varphi(k_{\mathrm{pf}} - 1)}{2 + k_{\mathrm{pf}} - \varphi(k_{\mathrm{pf}} - 1)}\right] \quad (8)$$

where k_{pf} is obtained from the following relationship [23]:

$$k_{\mathrm{pf}} = \frac{k_{\mathrm{p}}}{K_{\mathrm{f}}} \quad (9)$$

In the above relationships, φ represents the volume percentage of nanoparticles, index 'm' is associated with the properties of the nanofluid, index 'f' denotes the properties of the base fluid, and index 'p' indicates the properties of the nanoparticles.

Reynolds number is defined as follows:

$$\mathrm{Re} = \frac{\rho v d}{\mu} \quad (10)$$

2.2 Networking

To solve the problems numerically, it is essential to mesh the fluid and solid environment. To achieve this, the geometry is divided into smaller elements. The type and number of elements impact the accuracy, computational time, and convergence of the numerical solution. Therefore, it is crucial to employ the necessary precision in the meshing process. In this study, we utilize Comsol software for meshing the current problem. Cubic elements are more suitable for fluid analysis problems. An example of the meshing performed is depicted in Figure 2. The number and size of the elements will be discussed in the grid independence section. This is achieved through a trial and error process by repeatedly solving the problem with different grid sizes. Subsequently, the numerical solution was conducted using four grids of varying sizes.

Before conducting a thorough investigation, the reliability and accuracy of the system were confirmed and compared with Shah equation [23] and Parizi's work [21] for steady flow under constant flux boundary conditions, using water as the working fluid. The results in Figure 3 demonstrate good agreement with the predictions of Shah equation [23] and Parizi's work [21] at two Reynolds numbers of 930 and 1354.

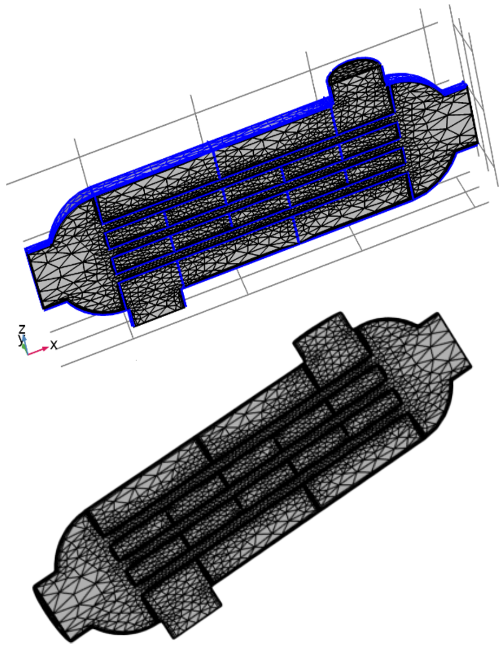

Fig. 2. A view of the mesh heat exchanger

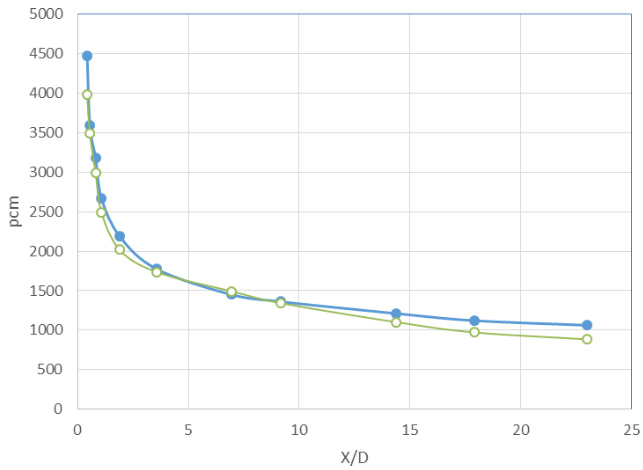

Fig. 3. Comparing the PCM results for the present study (blue filled circles) and Shah et al. [23] (hollow green circles).

Table 2. Computing nodes and meshing results

Number of cells	Number of nodes	PCM
2000	2145	2420/38
2820	3100	2420/41
6521	7260	2420/44
10900	110092	2420/48
11825	13297	2420/52

2.3 Explanations about the finite volume method

Well suited for the numerical simulation of various types of conservation laws, the finite volume method is a discretization method. In several engineering fields, such as fluid mechanics, heat and mass transfer, or petroleum engineering, the finite volume method has been extensively used. Like the finite element method, the finite volume method possesses important features. It may be used on arbitrary geometries, using structured or unstructured meshes, leading to robust schemes, as stated by Oden [22]. The numerical fluxes exhibit an additional feature, known as the local conservatively, where they are conserved from one discretization cell to its neighbor. In problems where the flux holds significant importance, such as in fluid mechanics, the finite volume method becomes highly appealing due to this particular feature.

3 Results

A heat exchanger is a specialized device that facilitates efficient heat transfer between two distinct regions, typically characterized by varying temperatures. It operates on the fundamental principles of thermal conductivity and phase changes of fluids. By employing well-engineered design techniques, a heat exchanger maximizes heat transfer efficiency, ensuring optimal performance in transferring heat from a hot area to a cold area. Figure 4 examines and compares the effect of changes in the heat exchanger speed on the forced heat transfer coefficient under constant heat flux.

First, the test has been conducted with two different Reynolds numbers, 877 and 945, using different materials. Figure 5 illustrates the displacement heat transfer coefficient in the exchanger tube. The results indicate that the use of ferrofluid enhances the displacement heat transfer. Additionally, it can be inferred from the graph that in shorter axial distances from the inlet, the increase in heat transfer is relatively more significant compared to larger distances where there is boundary layer disturbance. The transfer of particles, gradients in viscosity, and Brownian motion are factors contributing to the increased heat transfer in the fluid. The transfer of particles and turbulence in the thermal boundary layer is one of the most important factors in enhancing heat transfer. As a result, there is an increase in heat transfer.

The increase in the displacement heat transfer coefficient for turbulence flow under constant flux boundary conditions has been compared using water as the working fluid. The results are presented in Figure 6 for PCM and plain heat exchangers. The effect of the material has led to an increase in the displacement heat transfer coefficient, indicating the potential to enhance heat transfer using air and water materials, which further increases. The slowly moving fluid flow, as it travels through the pipe and interacts with the pipe wall, disrupts the thermal boundary layer, leading to an increase in the heat transfer coefficient for the displacement of the fluid flow.

Figure 7 illustrates the fluctuations in pressure within the converter tube. The findings indicate that including ferrofluid leads to an augmentation in the fluid pressure parameter. In various scenarios, the top section of the converter consistently reaches the highest temperature due to buoyancy effects compared to other regions. Through studying the impact of fin thickness, it has been observed that increasing the thickness of the fins reduces the time it takes for the PCM (paraffin) to melt. This improvement enhances energy storage capabilities (Figure 8).

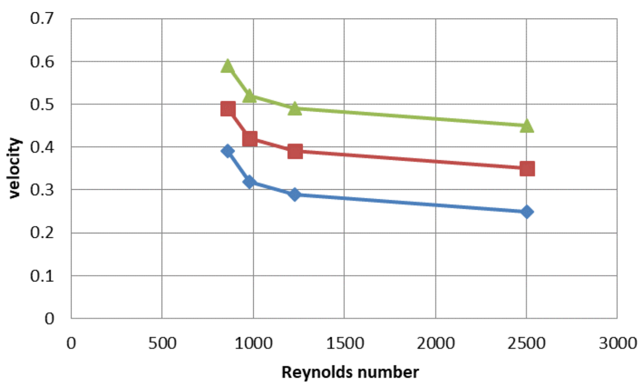

Fig. 4. Comparison of changes in heat exchanger velocity, displacement heat transfer coefficient in constant PCM heat flux: Re=1230 (upper line) , Re=980 (middle line), Re=877 (bottom line) .

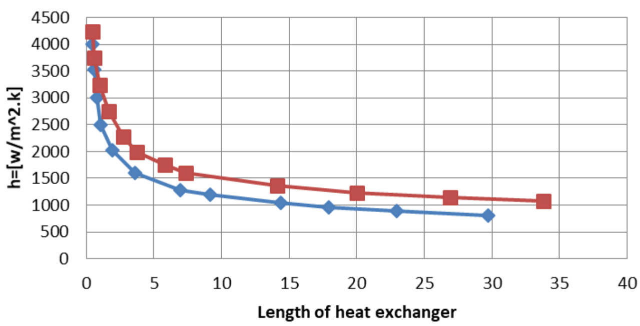

Fig. 5. Evaluation of numerical data of h increase with increasing Reynolds number in PCM shell and tube heat exchanger (Reynolds Water 945 [red squares]) and (Reynolds air 877 [blue diamonds]).

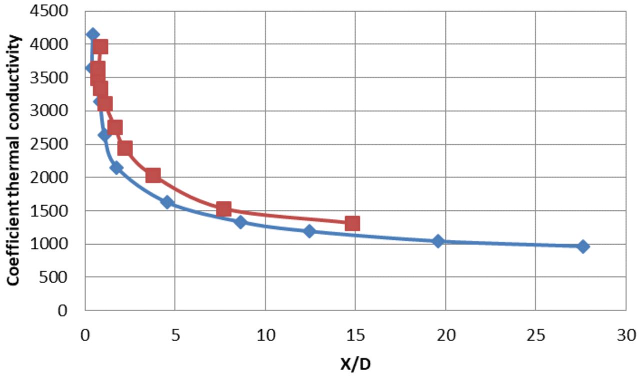

Fig. 6. Comparison of simple h increase with heat exchanger (Simple [blue diamonds]) and (Heat Exchanger [red squares]).

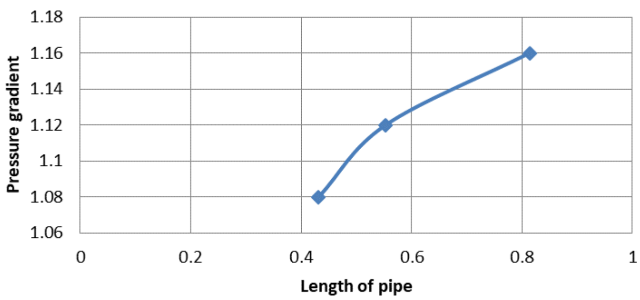

Fig. 7. PCM heat exchanger pressure changes

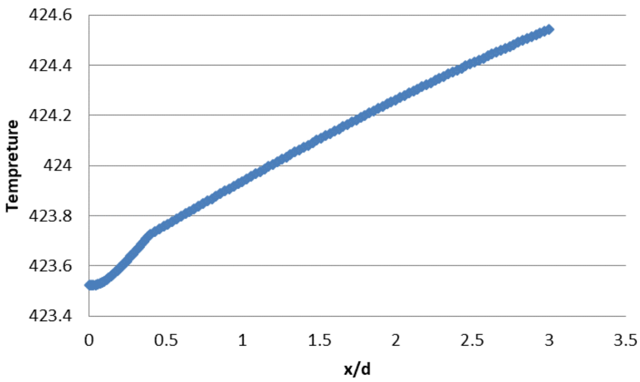

Fig. 8. PCM heat exchanger temperature changes

The comparison is made between the straight, circular tube and the shell and tube heat exchanger with increased transmittance coefficient while keeping the heat flux constant and using a PCM surrounding the tube. The selected fluid flow, having turbulence due to its motion and collision inside the tube, has disrupted the thermal boundary layer, leading to an increase in the internal transfer coefficient of the fluid flow (Figures 9 and 10).

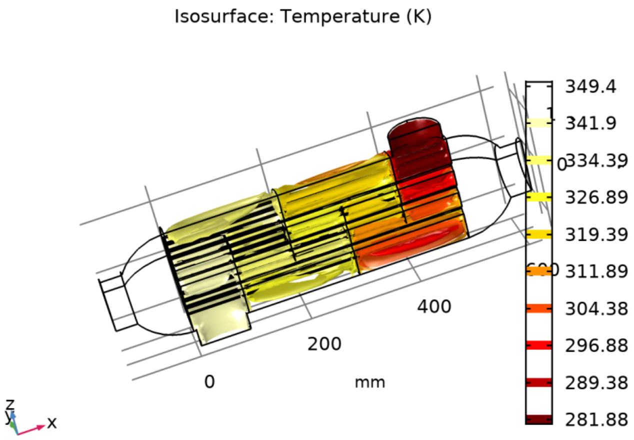

Fig. 9. Three-dimensional temperature heat transfer displacement heat exchanger under constant flux PCM

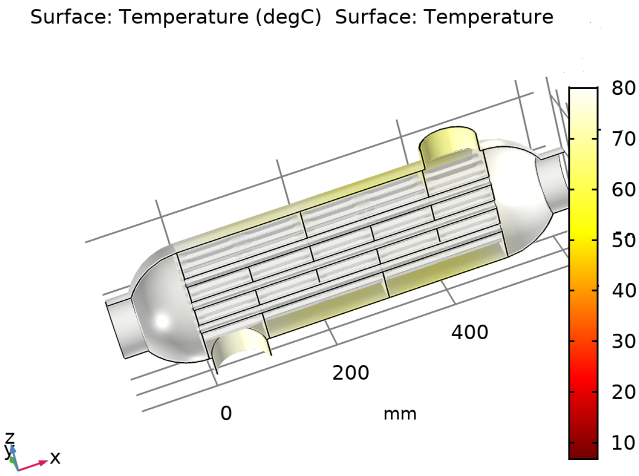

Fig. 10. Three-dimensional temperature changes of heat transfer displacement heat exchanger under constant flux PCM

Figure 11 depicts the changes in displacement heat transfer coefficients concerning Reynolds numbers for two nanofluids. To maximize thermal efficiency, two different nanofluids are compared in this graph. Silicon is not the best choice for increasing the heat transfer rate; instead, aluminum oxide nanoparticles are.

4 Conclusions

Focusing on investigating displacement heat transfer using (PCM), this article examines the three-dimensional flow and turbulence of water and air within a shell and tube heat exchanger. By utilizing the finite volume method, the fundamental equations governing the issue have been successfully resolved.

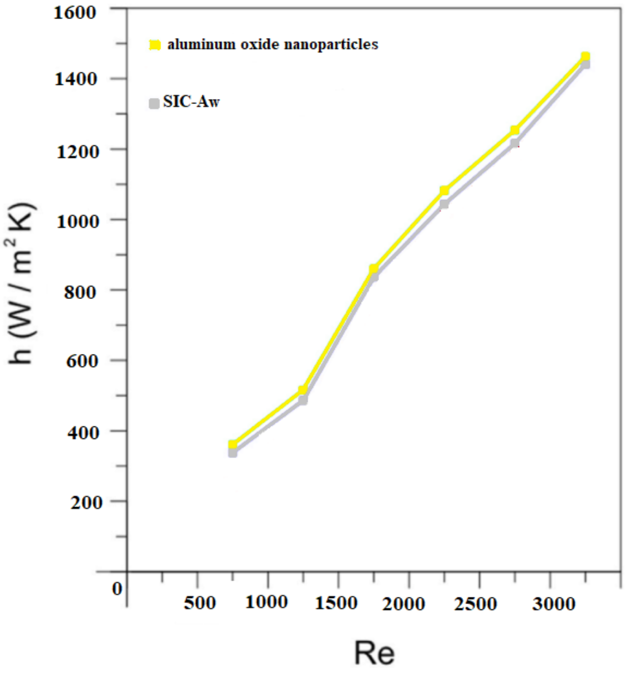

Fig. 11. Changes in heat transfer coefficient for two used nanofluids(aluminum oxide and SIC-Aw [25])

The study investigates the impact of increasing the penetration coefficient in a shell and tube heat exchanger while keeping the heat flux constant and incorporating a PCM around the tube. The results obtained shed light on this phenomenon:

- By increasing the penetration coefficient of the shell and tube heat exchanger and keeping the heat flux constant while placing PCM around the tube, a comparison was made between this setup and a straight, circular tube where fluid flow is selected by moving through the tube and colliding with the thermal boundary layer. It was observed that increasing the penetration coefficient led to disturbance in the thermal boundary layer, causing an increase in the internal transfer coefficient of the fluid flow. However, this resulted in an insignificant error of 8.71%.
- In all situations, the upper half of the converter has experienced the highest temperature due to buoyancy compared to other areas. By examining the effect of the fins' thickness, it was found that increasing the fins' thickness reduces the melting time of the PCM (paraffin), which improves Energy storage.
- In line with the topic of this article, future research can be directed toward obtaining temperature changes both around and within the heat exchanger. This can be achieved by modifying the length and pipe diameter of the heat exchanger, as well as altering the flow rate of the nanofluid entering the exchanger. Such modifications can lead to the discovery of new results.

Nomenclature

C_{pm}	Specific heat of ferrofluid (J/kg K)
d	Diameter of pipe (mm)
f	properties of the base fluid
$\boldsymbol{k}$	Unit vector for gravity (g)
K_m	Coefficient of ferrofluid thermal conductivity (W/mK)
m	Properties of the nanofluid
p	Pressure (Pa)
Re	Reynolds Number (Dimensionless)
S	Stress tensor (N/m^2)
T	Temperature (K)
u	Velocity in x direction (m/s)
v	Velocity in y direction (m/s)
η	Viscosity loss (Pa s)
β_m	Coefficient of thermal expansion (K^{-1})
φ	Volume percentage of nanoparticles (nm)
ρ	Density (kg/m^3)
μ	Dynamic viscosity (Pa s)
α	Thermal expansion coefficient (C^{-1})

References

[1] Alves TA, Altemani CA. Conjugate cooling of a discrete heater in laminar channel flow. Journal of the Brazilian Society of Mechanical Sciences and Engineering. 2011;33(3):278-86.

[2] Alves TA, Krambeck L, Santos Pd, Aranguren P. Heat pipe and thermosyphon for thermal management of thermoelectric cooling. Bringing thermoelectricity into reality. 2018.

[3] Wang S, He S, Wang M, Tian W, Su G, Qiu S. Two parallel methods for the three-dimensional CFD coupling simulation of shell and tube heat exchangers. Annals of Nuclear Energy. 2024;199:110374.

[4] Prajapati P, Raja BD, Savaliya H, Patel V, Jouhara H. Thermodynamic evaluation of shell and tube heat exchanger through advanced exergy analysis. Energy. 2024;292:130421.

[5] Amudhalapalli GK, Devanuri JK. Prediction of transient melt fraction in metal foam-nanoparticle enhanced PCM hybrid shell and tube heat exchanger: A machine learning approach. Thermal Science and Engineering Progress. 2023;46:102241.

[6] Gorzin M, Hosseini MJ, Rahimi M, Bahrampoury R. Nano-enhancement of phase change material in a shell and multi-PCM-tube heat exchanger. Journal of Energy Storage. 2019;22:88-97.

[7] Pahamli Y, Hosseini M, Ranjbar A, Bahrampoury R. Effect of nanoparticle dispersion and inclination angle on melting of PCM in a shell and tube heat exchanger. Journal of the Taiwan Institute of Chemical Engineers. 2017;81:316-34.

[8] Gasia J, Tay NS, Belusko M, Cabeza LF, Bruno F. Experimental investigation of the effect of dynamic melting in a cylindrical shell-and-tube heat exchanger using water as PCM. Applied energy. 2017;185:136-45.

[9] Hosseini M, Rahimi M, Bahrampoury R. Experimental and computational evolution of a shell and tube heat exchanger as a PCM thermal storage system. International Communications in Heat and Mass Transfer. 2014;50:128-36.

[10] Pahamli Y, Hosseini MJ, Ranjbar AA, Bahrampoury R. Analysis of the effect of eccentricity and operational parameters in PCM-filled single-pass shell and tube heat exchangers. Renewable energy. 2016;97:344-57.

[11] Zhang Z, Zhu Z. Optimum design of a horizontal shell-and-tube latent heat thermal energy storage system via non-uniform upper-and-lower cascade PCMs. Journal of Energy Storage. 2024;79:110209.

[12] Zaytoun MM, El-Bashouty MM, Sorour MM, Alnakeeb MA. Heat transfer characteristics of PCM inside a modified design of shell and tube latent heat thermal energy storage unit. Case Studies in Thermal Engineering. 2023;49:103372.

[13] Khedher NB, Hosseinzadeh K, Abed AM, Khosravi K, Mahdi JM, Sultan HS, et al. Accelerated charging of PCM in coil heat exchangers via central return tube and inlet positioning: a 3D analysis. International Communications in Heat and Mass Transfer. 2024;152:107275.

[14] Wu Y, Rong J, Wang D, Zhao X, Meng L, Arıcı M, et al. Synergistic enhancement of heat transfer and thermal storage characteristics of shell and tube heat exchanger with hybrid nanoparticles for solar energy utilization. Journal of Cleaner Production. 2023;387:135882.

[15] Sayehvand HO, Abolfathi S, Keshavarzian B. Investigating heat transfer enhancement for PCM melting in a novel multi-tube heat exchanger with external fins. Journal of Energy Storage. 2023;72:108702.

[16] Boujelbene M, Mohammed HI, Sultan HS, Eisapour M, Chen Z, Mahdi JM, et al. A comparative study of twisted and straight fins in enhancing the melting and solidifying rates of PCM in horizontal double-tube heat exchangers. International Communications in Heat and Mass Transfer. 2024;151:107224.

[17] Conti M, Charach C. Thermodynamics of heat storage in a PCM shell-and-tube heat exchanger in parallel or in series with a heat engine. Solar energy. 1996;57(1):59-68.

[18] Chandran KN, Jeong YS, Kim HG, Min JK, Ha MY. Investigation of the thermal exchange mechanism of PCM melting process in an LHTES with elliptic tube configurations inside a cylindrical shell. Journal of Energy Storage. 2024;76:109838.

[19] Yang X, Lu Z, Bai Q, Zhang Q, Jin L, Yan J. Thermal performance of a shell-and-tube latent heat thermal energy storage unit: Role of annular fins. Applied energy. 2017;202:558-70.

[20] Said MA, Hosseinzadeh K, Kaplan S, Rahbari A, Tiji ME, Mahdi JM, et al. Accelerated charging dynamics in shell-and-multi-tube latent heat storage systems for building applications. Journal of Energy Storage. 2024;81:110286.

[21] Dhshiri Parizi A, Salimpour MR. Water/TiO2 nanofluid flow heat transfer and pressure drop through ducts with circular, square and rectangular cross-sections. Modares Mechanical Engineering. 2015;15(5):377-82. Available from: https://mme.modares.ac.ir/article_8651.html.

[22] Kikuchi N, Oden JT. Contact problems in elasticity: a study of variational inequalities and finite element methods. SIAM; 1988.

[23] Shah R, Heikal M, Thonon B, Tochon P. Progress in the numerical analysis of compact heat exchanger surfaces. In: Advances in heat transfer. vol. 34. Elsevier; 2001. p. 363-I.

[24] He Z, Li R, Yang L, Mikulčić H, Wang J, Čuček L. Performance analysis of a battery thermal management system based on phase change materials with micro heat pipe arrays. Energy conversion and management. 2024;311:118506.

[25] Karuppusamy S, Sambandam P, Selvaraj M, Kaliyaperumal G, Mariadhas A, Deepak J. Enhancing heat transfer efficiency in shell-and-tube heat exchangers with SiC and CNT-infused alkaline water nanofluids. Desalination and Water Treatment. 2024;317:100157.